Chapter 2
From the Mathematical Model to the Circuit

Abstract Starting from the mathematical model of a nonlinear system, it is always possible to realize an electronic circuit, which is equivalent to the mathematical model, in the sense that it obeys to the same set of equations. In this chapter, the approach for designing the electronic circuit, equivalent to a given mathematical model, is illustrated.

Keywords Chaotic circuits · Design guidelines · Operational amplifier

2.1 Building Blocks

This section summarizes the basic blocks needed for the realization of an electronic circuit equivalent to a nonlinear system.

2.1.1 Operational Amplifier

The main building block for nonlinear circuits is the operational amplifier (OP-AMP). OP-AMPs are electronic devices important for a wide range of applications [1]. They are characterized by two differential inputs V_+ and V_- and one output V_{out}. The circuital symbol used is shown in Fig. 2.1, where the power supplies are indicated as $-V_{\text{cc}}$ and V_{cc}. The transfer characteristic of the OP-AMP from input to the output is nonlinear and can be expressed as follows:

$$V_{\text{out}} = f(v_d) = \begin{cases} -E_{\text{sat}} & v_d \leq -\frac{E_{\text{sat}}}{A_v} \\ A_v v_d & -\frac{E_{\text{sat}}}{A_v} < v_d < \frac{E_{\text{sat}}}{A_v} \\ E_{\text{sat}} & v_d \geq \frac{E_{\text{sat}}}{A_v} \end{cases} \tag{2.1}$$

A. Buscarino et al., *A Concise Guide to Chaotic Electronic Circuits*,
SpringerBriefs in Applied Sciences and Technology,
DOI: 10.1007/978-3-319-05900-6_2, © The Author(s) 2014

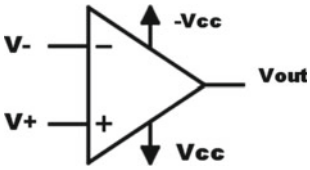

Fig. 2.1 Symbol of the operational amplifier

where:

- E_{sat} is the voltage value at which the output of the operational amplifier saturates. It depends on the internal circuitry design of the device and on the voltage supply used. The region in which $V_{\text{out}} = A_v v_d$ is defined as the linear region;
- $v_d = V_- - V_+$, is the voltage between the two terminals V_+ and V_-.

In the ideal case, the device has high input impedance, low output impedance and a high voltage gain A_v. As a consequence of the high input impedance, no current flows into or out of the input terminals. An operational amplifier can be integrated in a single chip and used to implement several types of mathematical operations according to the specific configuration. We will discuss the following configurations needed in the design procedure:

1. inverting configuration;
2. non-inverting configuration;
3. algebraic adder;
4. RC integrator;
5. Miller integrator.

2.1.2 Inverting Configuration

In Fig. 2.2 the inverting configuration is shown. An inverting amplifier uses negative feedback to amplify the input voltage while changing its sign. The output v_{out} is related to the input v_{in} through the following equation:

$$V_{\text{out}} = -\frac{R_2}{R_1} V_{\text{in}} \tag{2.2}$$

where the gain is fixed by the ratio between R_2 and R_1.

This relationship can be derived by taking into account that the current i flowing into the resistor R_1 is given by:

$$i = \frac{V_{\text{in}} + v_d}{R_1} \tag{2.3}$$

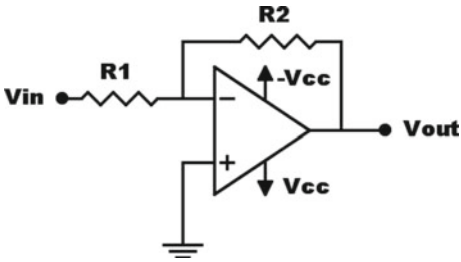

Fig. 2.2 Inverting configuration of the operational amplifier

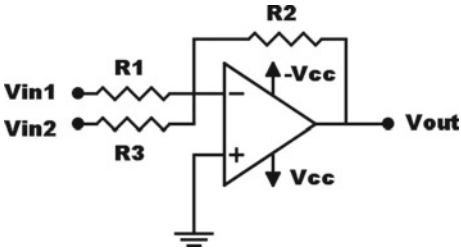

Fig. 2.3 Inverting adder configuration of the operational amplifier

Since no current flows in the negative input terminal, because of the high impedance of this node, the current in R_2 is the same in R_1, and thus:

$$V_{\text{out}} = -R_2 i + v_d \tag{2.4}$$

It is possible to derive that:

$$V_{\text{out}} = -\frac{R_2}{R_1} V_{\text{in}} - \left(\frac{R_2}{R_1} + 1\right) v_d \tag{2.5}$$

and considering that, usually, the device works in the linear region, one gets:

$$\frac{V_{\text{out}}}{V_{\text{in}}} = -\frac{\frac{R_2}{R_1} A_v}{A_v + \left(\frac{R_2}{R_1} + 1\right)} \tag{2.6}$$

In the limit of large gain, $A_v \to \infty$, the relationship (2.2) is obtained. An inverting adder is built from this basic configuration by considering more than one input. The scheme is shown in Fig. 2.3. In the limit of large gain the output is given by:

$$V_{\text{out}} = -\frac{R_2}{R_1} V_{\text{in1}} - \frac{R_2}{R_3} V_{\text{in2}} \tag{2.7}$$

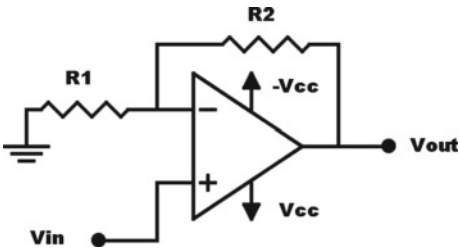

Fig. 2.4 Non-inverting configuration of the operational amplifier

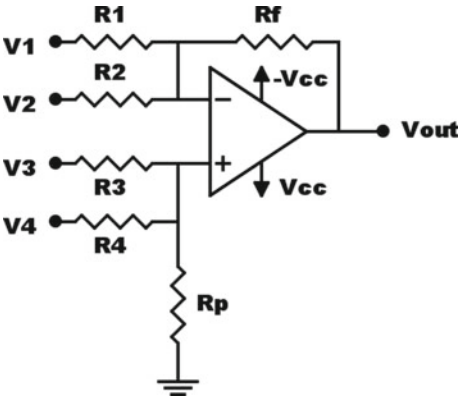

Fig. 2.5 Algebraic adder configuration of the operational amplifier

2.1.3 Non-inverting Configuration

In Fig. 2.4 the non-inverting configuration is shown. A non-inverting amplifier realizes an amplification of the input voltage. By following considerations similar to what taken into account for the inverting configuration, it can be demonstrated that, in this case, the output V_{out} is given by:

$$V_{\text{out}} = \left(\frac{R_2}{R_1} + 1\right) V_{\text{in}} \tag{2.8}$$

2.1.4 Algebraic Adder Configuration

The equations of a nonlinear system often include the sum of more than one term. So, the need of implementing a mathematical operation like an algebraic sum arises. To do this, an algebraic adder circuit configuration is used. The scheme is reported in Fig. 2.5. It implements the following mathematical operation:

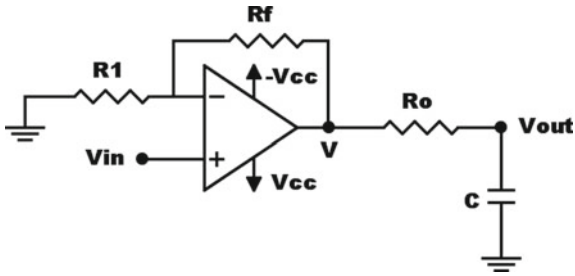

Fig. 2.6 RC integrator

$$V_{\text{out}} = -\frac{R_f}{R_1}V_1 - \frac{R_f}{R_2}V_2 - \frac{R_f}{R_3}V_3 - \frac{R_f}{R_4}V_4 \tag{2.9}$$

The value of the resistor R_p is fixed in order to satisfy the following equation (sometime referred as the *gain rule*):

$$\frac{1}{R_1} + \frac{1}{R_2} = \frac{1}{R_3} + \frac{1}{R_4} + \frac{1}{R_p} \tag{2.10}$$

which, essentially, requires that the sum of the conductances at the inverting terminal of the operational amplifier equals that at the negative terminal. Under this assumption, the output of the circuit is given by the following equation:

$$V_{\text{out}} = \sum_i A_i V_i \tag{2.11}$$

with $A_i = \frac{R_f}{R_i}$. The output depends on each single input by means of only the associated input resistor and not of the other resistors, which is very convenient from the designer perspective. We notice that, when satisfying the gain rule results in a negative value of R_p, another resistance connected to ground should be added at the negative input of the OP-AMP.

2.1.5 RC Integrator

Another important mathematical operation required in the derivation of equivalent electronic circuits is realized by the integrator configuration that exploits the properties of the operational amplifier in the linear region. The configuration is shown in Fig. 2.6.

Assuming that the node V_{out} is connected to an high impedance, the current flowing in the resistor R_o can be considered equal to that in the capacitor. The current flowing into the resistor R_o is:

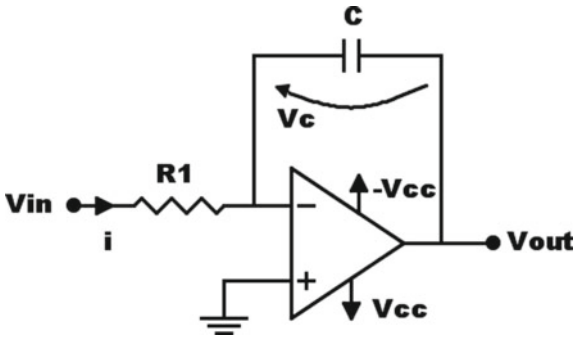

Fig. 2.7 Miller integrator

$$i = \frac{V - V_{\text{out}}}{R_o} \tag{2.12}$$

On the other hand, taking into account the relationship between current and voltage across the capacitor, one gets:

$$i = C\frac{\mathrm{d}V_{\text{out}}}{\mathrm{d}t} \tag{2.13}$$

$$CR_o\dot{V}_{\text{out}} = -V_{\text{out}} + AV_{\text{in}} \tag{2.14}$$

Thanks to the relationship in Eq. (2.14) and provided that the input V_{in} is appropriately selected, a base block implementing a first-order generic differential equation of the type:

$$\dot{x} = k(-x + f(x,t)) \tag{2.15}$$

may be realized with $k = \frac{1}{CR_o}$.

2.1.6 Miller Integrator

The Miller integrator is another circuit which allows to obtain an output corresponding to the integral of the input signal. The scheme of the circuit is shown in Fig. 2.7.

This configuration is similar to the inverting configuration of Fig. 2.2, where the resistance R_2 has been replaced by the capacitor C. Considering an ideal operational amplifier, the current in the resistor R_1 and that in the capacitor C are equal, the voltage difference between the inverting and non-inverting terminals is equal to zero and the inverting terminal is connected to virtual ground. The current flowing in R_1 is:

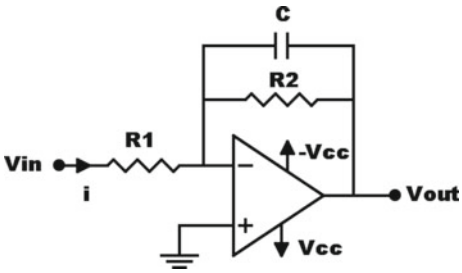

Fig. 2.8 Miller integrator with feedback resistor

$$i = \frac{V_{\text{in}}}{R_1} \tag{2.16}$$

and, since

$$i = C\frac{\mathrm{d}V_c}{\mathrm{d}t} \tag{2.17}$$

and $V_{\text{out}} = -V_c$, one has:

$$CR_1\dot{V}_{\text{out}} = -V_{\text{in}}. \tag{2.18}$$

The drawback of the circuit of Fig. 2.7 is that it can easily go into saturation, due to low frequency noise or offsets; in fact, if the frequency of the noise tends to zero, the reactance of the capacitor C tends to infinity and so the capacitor becomes an open circuit and its amplification is therefore infinite, so reaching the saturation.

To avoid this, a resistor is inserted in parallel to the capacitor, as shown in Fig. 2.8, so that the maximum gain of the operational amplifier is limited to the value $A_v = -\frac{R_2}{R_1}$. The resistance R_2 must be selected so that at the working frequency of the integrator the presence of the resistance is negligible (that is, the resistance is larger than) with respect to the reactance of the capacitor:

$$\frac{1}{\omega C} \gg R_2 \tag{2.19}$$

where $\omega = 2\pi f$ and f is the working frequency of the integrator.

2.1.7 The Analog Multiplier AD633

Many chaotic circuits have polynomial nonlinearities or products of state variables. Electronic realization of the product operation may be carried out with the AD633 analog component. This is a low-cost multiplier with the functional block diagram of Fig. 2.9.

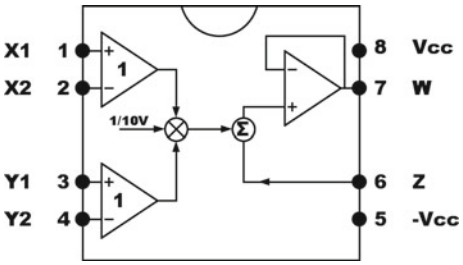

Fig. 2.9 Functional block diagram of the analog multiplier AD633

The output of AD633 is related to its input through:

$$W = \frac{(X1 - X2)(Y1 - Y2)}{10\,\mathrm{V}} + Z. \tag{2.20}$$

2.1.8 PWL Approximation of Nonlinearities

The approach based on analog multipliers may be expensive for higher order nonlinearities, thus requiring the cascade of two or more multipliers, or when many chaotic circuits have to be realized. Alternatively, it is possible to use an approach based on piecewise linear (PWL) functions. The idea is to derive a PWL approximation of the nonlinearity to be implemented, to realize a circuitry with the PWL given characteristics, and then to use it instead of the multipliers in the implementation of the circuit. In fact, it has been demonstrated that a wide class may be approximated by using only piecewise linear functions [2]. The design of such PWL functions, and in particular the number of segments, depends on the desired accuracy and on the dynamical range in which the approximation holds. The circuitry implementing the PWL functions is realized with a few components, including diodes to implement the segment breakpoints.

Two examples of circuits that will then be used in Chap. 3 are given here. They both properly work with inputs in the dynamic range of ± 3 V. A circuit whose output is the square of the input signal is reported in Fig. 2.10, while Fig. 2.11 implements a PWL approximation of a circuit whose output is the cube of the input signal. For low-cost implementations, these two circuits are more convenient than circuits based on the multiplier $AD633$ since they contain only diodes, resistors, and operational amplifiers.

2.1.9 Negative Resistance

In Fig. 2.12 the symbol and an electronic circuit that can be used as a negative resistance are shown. A brief explanation of the principles of the circuit is reported below. Considering the operational amplifier with ideal characteristics:

$$V_{\mathrm{nr}} = R_1 i + V_o \tag{2.21}$$

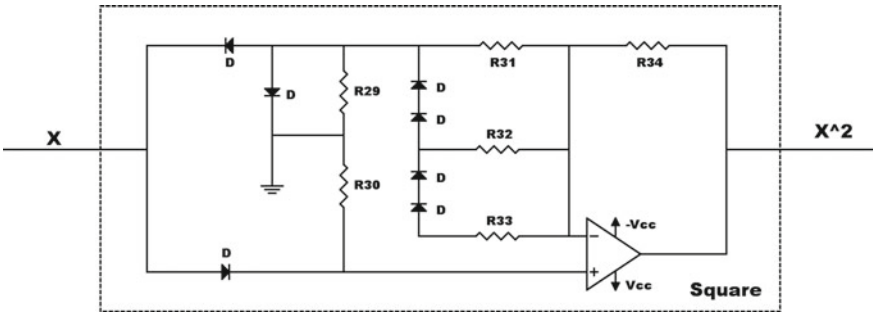

Fig. 2.10 Circuital implementation of the square function. Components: $R_{29} = 10\,\text{k}\Omega$, $R_{30} = 10\,\text{k}\Omega$, $R_{31} = 10\,\text{k}\Omega$, $R_{32} = 10\,\text{k}\Omega$, $R_{33} = 4\,\text{k}\Omega$, $R_{34} = 30\,\text{k}\Omega$, $1N4148$ Diode, $V_{\text{cc}} = 9\,\text{V}$

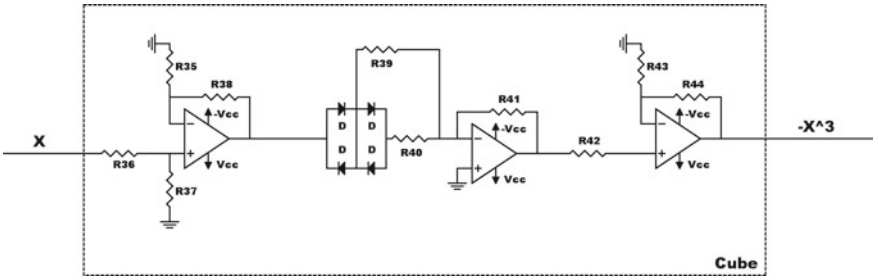

Fig. 2.11 Circuital implementation of the cube function. Components: $R_{35} = 200\,\text{k}\Omega$, $R_{36} = 200\,\text{k}\Omega$, $R_{37} = 100\,\text{k}\Omega$, $R_{38} = 100\,\text{k}\Omega$, $R_{39} = 12\,\text{k}\Omega$, $R_{40} = 2\,\text{k}\Omega$, $R_{41} = 15\,\text{k}\Omega$, $R_{42} = 10\,\text{k}\Omega$, $R_{43} = 10\,\text{k}\Omega$, $R_{44} = 70\,\text{k}\Omega$, $1N4148$ Diode, $V_{\text{cc}} = 9\,\text{V}$

Fig. 2.12 Symbol and circuital implementation of a negative resistance

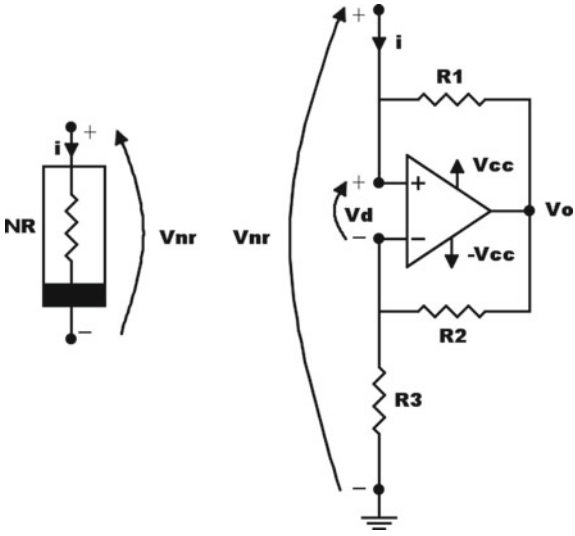

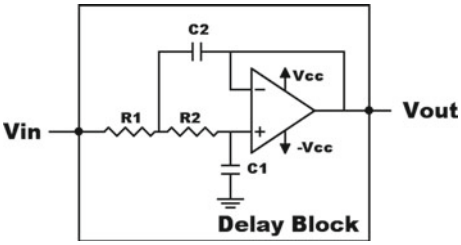

Fig. 2.13 The time-delay block. Schematics of the Sallen-Key low-pass active filter implementing a low-pass Bessel filter. Component values: $R_1 = 10\,\text{k}\Omega$, $R_2 = 10\,\text{k}\Omega$, $C_1 = 10\,\text{nF}$, $C_2 = 22\,\text{nF}$, $V_{\text{cc}} = 9\,\text{V}$

and

$$V_{\text{nr}} = V_o \frac{R_3}{R_2 + R_3} + v_d. \tag{2.22}$$

Considering $v_d = 0$, from the relationship (2.22) we get

$$V_o = \frac{R_2 + R_3}{R_3} V_{\text{nr}}. \tag{2.23}$$

Substituting V_o in Eq. (2.21) we obtain:

$$V_{\text{nr}} = R_1 i + \frac{R_2 + R_3}{R_3} V_{\text{nr}} \tag{2.24}$$

from which, considering $R_1 = R_2$, we get:

$$V_{\text{nr}} = -R_3 i \tag{2.25}$$

which represents the $i - v$ relationship of the negative resistance.

2.1.10 Time-Delay Block

Another element which is worth to discuss is the time-delay block: in fact, there are nonlinear systems where the presence of a time-delay is fundamental to have chaos [3, 4]. The time-delay block may be implemented by using a cascade of elementary time-delay blocks, where each elementary block is implemented by using a low-pass second-order Bessel filter. Each filter is implemented through the Sallen-Key topology shown in Fig. 2.13 and it is characterized by the following transfer function:

$$H(s) = \frac{1}{1 + C_1(R_1 + R_2)s + C_1 C_2 R_1 R_2 s^2}. \tag{2.26}$$

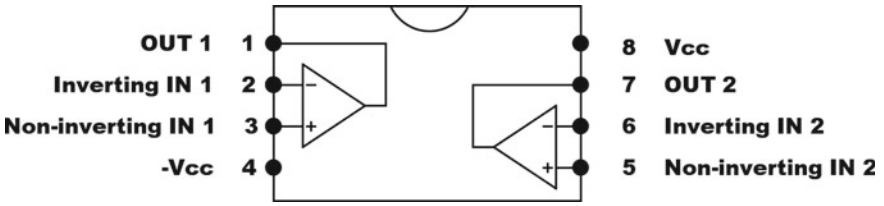

Fig. 2.14 TL082 functional block diagram

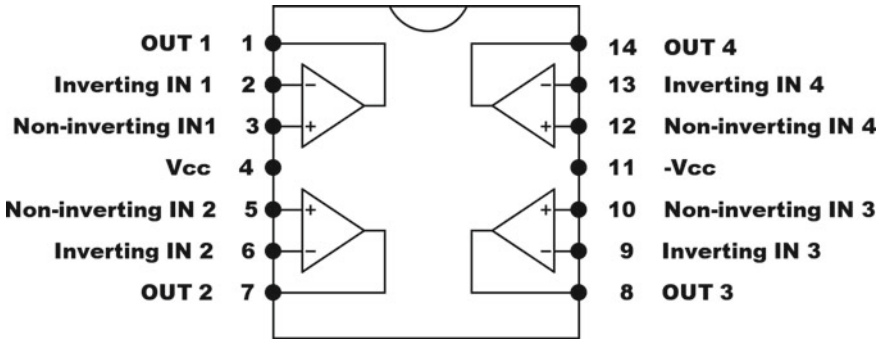

Fig. 2.15 TL084 functional block diagram

The values of the filter components have been chosen in order to realize a Bessel filter with 3 dB frequency equal to $f_c \approx 1$ kHz and taking into account off-the-shelf component values. The time-delay introduced by this filter in the band up to 3 dB can be calculated as $\tau = C_1(R_1 + R_2) = 0.219$ ms. Larger delays are realized by taking into account a cascade of n filters.

2.1.11 General Purpose Amplifiers

TL082 and TL084 are low cost, high speed operational amplifiers. They require low supply voltage, yet maintaining a large gain bandwidth. For this reason, the circuits discussed in the next chapter use such devices. The difference between TL082 and TL084 relies in the number of operational amplifiers integrated in the chip, as apparent from the functional block diagrams of Figs. 2.14 and 2.15. The TL082 has only two operational amplifiers while the TL084 has four.

2.2 Methodology

In this section the methodology to design equivalent electronic circuits starting from a mathematical model is discussed. The mathematical model is expressed in the form

$$\dot{x} = f(x, t) \tag{2.27}$$

where $x \in R^n$, $f : R^n \rightarrow R^n$ and $\dot{x} = \frac{dx}{dt}$. The system in Eq. (2.27) is rewritten as:

$$\dot{x} = -x + Ax + g(x) \tag{2.28}$$

where the linear part and the nonlinear part of the system are emphasized. To each equation of the set of Eq. (2.28) a RC integrator equation in the following form may be associated:

$$\dot{x}_i = -x_i + h_i(x) \tag{2.29}$$

where $h_i(x) = \sum_j a_{ij}x_j + g_i(x)$. To implement $h_i(x)$ an algebraic adder that realizes $\sum_j a_{ij}x_j$, and $g_i(x)$ and then a nonlinear block that implement $g_i(x)$ are needed.

The design of an equivalent nonlinear circuit starting from a set of ordinary differential equations follows three steps.

First step

Any mathematical model, which is the basis of a dynamical system, has a number of state variables following a particular temporal trend. These trends are within a range which depends on the model and its parameters.

In order to implement the model with an electronic circuit using standard circuital components (resistors, capacitors, operational amplifiers, etc.), it is important that the oscillations of the state variables are confined within the limits imposed by the voltage supplies powering the operational amplifiers (otherwise, undesired saturations may be reached). To establish the specific power supply voltage, it is necessary to examine the model using simulation tools. If there are state variables or linear or nonlinear combinations of these which are outside the range of the limits imposed by the voltage supplies, the system in Eq. (2.29) must be rescaled in amplitude, using a transformation of the type:

$$\mathbf{X} = \mathbf{kx} \tag{2.30}$$

where $\mathbf{X} \in R^n$, $\mathbf{x} \in R^n$, and $\mathbf{k} = \begin{bmatrix} k_1 & 0 & \cdots & 0 \\ 0 & k_2 & \cdots & 0 \\ \vdots & \vdots & \ddots & \vdots \\ 0 & 0 & \cdots & k_n \end{bmatrix}$ where $k_1, k_2, \ldots, k_n$ are real quantities. To check the limits of the oscillations and those of the rescaled variables numerical simulations are performed. The numerical integration of the mathematical model is done by using a solver of ordinary differential equations, as for instance one of those provided in the software *MATLAB*®. In this first phase, the oscillation range and the operating frequencies are characterized. However, if the state variables oscillate outside physically realizable voltage limits, the system has to be suitably scaled in amplitude through the mathematical transformation (2.30) by appropriately selecting **k**.

The time variable of the dynamical system can also be rescaled by defining a new time variable as $\tau = \kappa t$. According to this Eq. (2.27) is rewritten as

$$\frac{\mathrm{d}x}{\mathrm{d}\tau} = \kappa f(x, \tau) \tag{2.31}$$

By comparing Eq. (2.31) with Eq. (2.15), we derive that the time scaling factor in the RC integrator is fixed by the product of capacitor C and resistor R_o as $\kappa = \frac{1}{CR_o}$. When n RC blocks are used in the circuit to implement the n state variables, all the capacitors and resistors of the blocks are chosen to match the same scaling factor. The same considerations apply to the Miller integrator. The temporal rescaling is introduced to reduce the observation time of the electrical waveforms.

Second step
In this step, the circuit is designed and simulated according to the observations made during the previous analysis, checking the feasibility of the designed circuit. $PSPICE^{®}$, $LTSpice$, and other circuital simulation environments provide a variety of custom circuit simulation tools to quickly and easily evaluate the designed circuit. In this second phase, the circuit, if well designed, will be checked to evaluate if it works as expected from the analysis carried on in the first phase of the procedure.

Third step
Finally, the circuit is physically implemented and experimentally characterized. The range of operating frequencies of each state variable is an important parameter of the system for both the feasibility and the ability to simultaneously acquire the trend of the state variables of the circuit. The acquisition of waveforms generated by the circuits, in fact, is a necessary practice that is performed in order to analyze in more detail the individual behavior of all the state variables and compare them with the theoretical trends that have been obtained in the numerical simulations.

2.3 An Example: The Rössler System

The Rössler system is one of the most well-known autonomous nonlinear systems that exhibit a chaotic attractor [5]. In terms of dimensionless equations the Rössler system is described by

$$\begin{cases} \dot{x} = -y - z \\ \dot{y} = x + ay \\ \dot{z} = b + z(x - c) \end{cases} \tag{2.32}$$

where

$$a = 0.2; \qquad b = 0.2; \qquad c = 7.0 \tag{2.33}$$

are parameter values for which a chaotic attractor appears (other values, however, also leading to chaotic behavior, are possible). In the following, the three steps of the methodology for the design of an electronic circuit equivalent to the Rössler system are applied to Eq. (2.32) to illustrate the procedure.

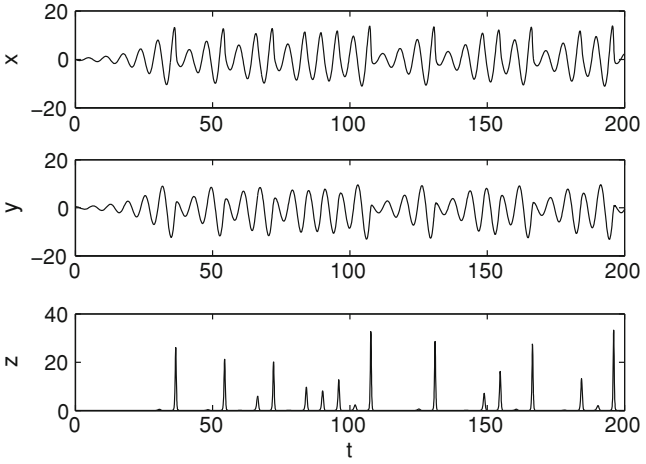

Fig. 2.16 Numerical simulations of Eq. (2.32): trend of the state variables x, y and z

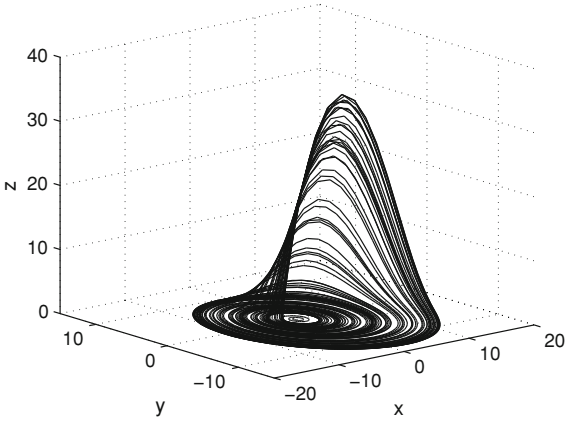

Fig. 2.17 Numerical simulations of Eq. (2.32): chaotic attractor

First step

Using *MATLAB*® and the mathematical model in Eq. (2.32) we analyze the temporal trends of the three state variables x, y, z, in particular paying attention to the amplitude range inside which each state variable oscillates. Figure 2.16 shows the behavior of the variables x, y, and z. In Fig. 2.17 the typical chaotic attractor of the Rössler system is shown. The plot is obtained by using the parameters (2.33). The ranges inside which x, y, and z oscillate, are the following:

$$x \in (-20, 20); \qquad y \in (-15, 15); \qquad z \in (0, 40) \tag{2.34}$$

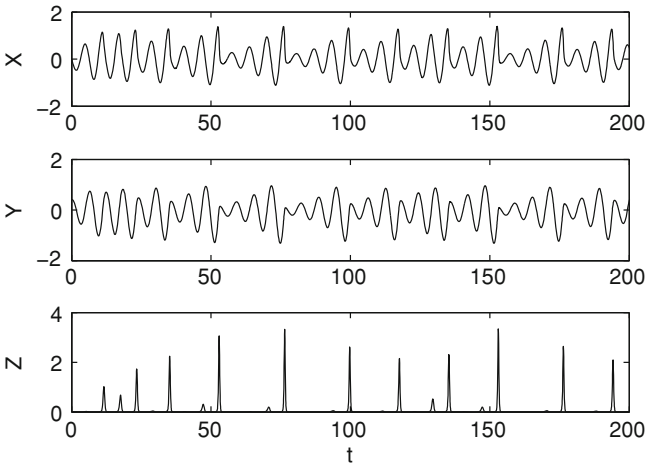

Fig. 2.18 Numerical simulations of Eq. (2.37): trend of the state variables X, Y and Z

If we use common 9 V batteries, these intervals are too large, so the system in Eq. (2.32) must be rescaled in amplitude. Design choices lead us to choose the scale factors as follows:

$$X = k_1 x; \qquad Y = k_2 y; \qquad Z = k_3 z \tag{2.35}$$

where

$$k_1 = \frac{1}{10}; \qquad k_2 = \frac{1}{10}; \qquad k_3 = \frac{1}{10}. \tag{2.36}$$

In this way a new rescaled equivalent system is found:

$$\begin{cases} \dot{X} = -Y - Z \\ \dot{Y} = X + aY \\ \dot{Z} = \frac{b}{10} + 10XZ - cZ. \end{cases} \tag{2.37}$$

The new rescaled system is now simulated and the trends of the state variables are verified to oscillate inside voltage limits that are now realizable. In this way, the feasibility of the circuit is checked (Figs. 2.18 and 2.19).

Second step

In this step, using operational amplifiers, resistors, capacitors, and other electronic components an equivalent electronic circuit is designed and then simulated with a circuital simulator to verify that the trends of the state variables are consistent with the numerical simulations analyzed before.

We start discussing the part of the circuit associated to the first rescaled equation

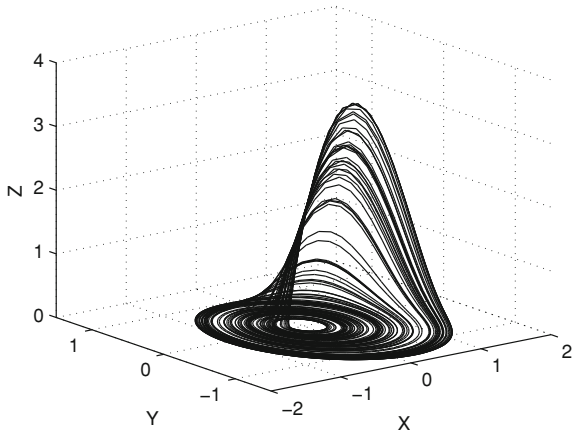

Fig. 2.19 Numerical simulations of Eq. (2.37): chaotic attractor

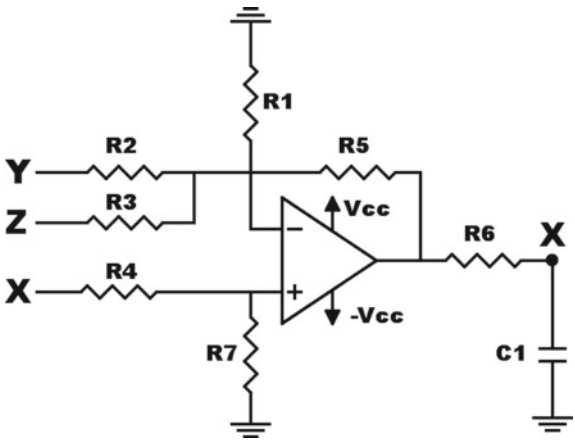

Fig. 2.20 Scheme of the circuit associated to the first rescaled Rössler equation. Parameters are: $R_1 = 100\,\mathrm{k}\Omega$, $R_2 = 100\,\mathrm{k}\Omega$, $R_3 = 100\,\mathrm{k}\Omega$, $R_4 = 100\,\mathrm{k}\Omega$, $R_5 = 100\,\mathrm{k}\Omega$, $R_6 = 1\,\mathrm{k}\Omega$, $R_7 = 33.3\,\mathrm{k}\Omega$, $C_1 = 100\,\mathrm{nF}$, $V_{\mathrm{cc}} = 9\,\mathrm{V}$

$$\dot{X} = -Y - Z. \tag{2.38}$$

The implementation of this equation needs one RC integrator and an adder. To the aim of using the RC integrator, the equation is rewritten in the form (2.15):

$$\dot{X} = -X + X - Y - Z. \tag{2.39}$$

Starting from this equation and keeping in mind the gain rule (2.10), we derive the circuit scheme of Fig. 2.20. Off-the-shelf resistors and capacitors, each with its own tolerance, are chosen as reported in the caption of Fig. 2.20. The choice of C_1 and R_6 fixes the time rescaling as $\kappa = \frac{1}{R_6 C_1} = 10000$. The circuit obeys the equation:

$$C_1 R_6 \dot{X} = -X + \frac{R_5}{R_4} X - \frac{R_5}{R_2} Y - \frac{R_5}{R_3} Z. \tag{2.40}$$

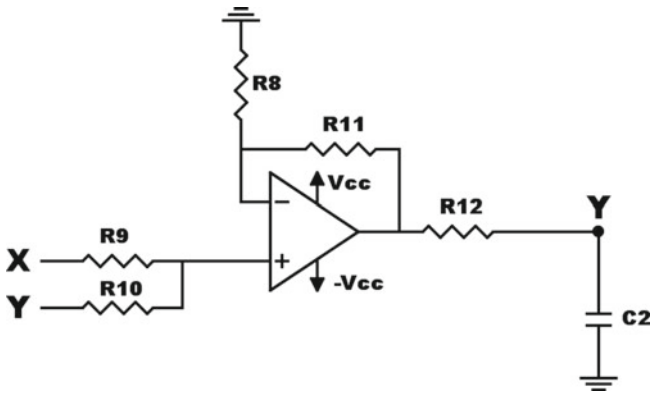

Fig. 2.21 Scheme of the circuit associated to the second rescaled Rössler equation. Parameters are: $R_8 = 78\,\mathrm{k}\Omega$, $R_9 = 100\,\mathrm{k}\Omega$, $R_{10} = 78\,\mathrm{k}\Omega$, $R_{11} = 100\,\mathrm{k}\Omega$, $R_{12} = 1\,\mathrm{k}\Omega$, $C_2 = 100\,\mathrm{nF}$, $V_{\mathrm{cc}} = 9\,\mathrm{V}$

In a similar way, we proceed for the other two state variables. The second rescaled equation is rewritten as:

$$\dot{Y} = -Y + X + (a+1)Y. \tag{2.41}$$

The scheme of the circuit is reported in Fig. 2.21 and the associated circuital equation as the following:

$$C_2 R_{12} \dot{Y} = -Y + \frac{R_{11}}{R_9} X + \frac{R_{11}}{R_{10}} Y. \tag{2.42}$$

Finally, the third rescaled equation is dealt with. The associated equation is rewritten as:

$$\dot{Z} = -Z + \frac{b}{10} + 10XZ + Z(1-c). \tag{2.43}$$

In this equation two new types of terms appear, a constant term $\frac{b}{10}$ and a nonlinear term XY. To implement the first term a voltage divider is used. The second term is realized through the analog multiplier AD633, as shown in Fig. 2.22, taking into account that the output is given by:

$$W = \frac{(X_1 - X_2)(Y_1 - Y_2)}{10\,\mathrm{V}} \frac{R_{22} + R_{23}}{R_{22}}. \tag{2.44}$$

So, if we select

$$X1 = X, \qquad X2 = 0, \qquad Y1 = Y, \qquad Y2 = 0 \tag{2.45}$$

and the ratio $\frac{R22+R23}{R22} = 10$, we obtain the term XZ. In summary, the third circuit equation is the following:

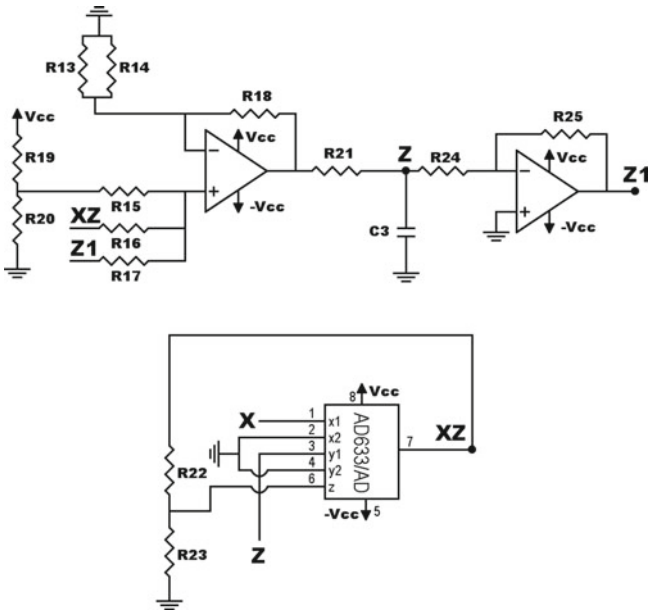

Fig. 2.22 Scheme of the circuit associated to the third rescaled Rössler equation. Parameters are: $R_{13} = 100\,\text{k}\Omega$, $R_{14} = 10\,\text{k}\Omega$, $R_{15} = 100\,\text{k}\Omega$, $R_{16} = 10\,\text{k}\Omega$, $R_{17} = 100\,\text{k}\Omega$, $R_{18} = 100\,\text{k}\Omega$, $R_{19} = 449\,\text{k}\Omega$, $R_{20} = 1\,\text{k}\Omega$, $R_{21} = 1\,\text{k}\Omega$, $R_{22} = 1\,\text{k}\Omega$, $R_{23} = 9\,\text{k}\Omega$, $R_{24} = 10\,\text{k}\Omega$, $R_{25} = 80\,\text{k}\Omega$ (potentiometer), $C_3 = 100\,\text{nF}$, $V_{\text{cc}} = 9\,\text{V}$

$$C_3 R_{21} \dot{Z} = -Z + \frac{R_{18} R_{25}}{R_{17} R_{24}} Z + \frac{R_{18}}{R_{16}} XZ + \frac{R_{18}}{R_{15}} \frac{R_{20}}{R_{19} + R_{20}} V_{\text{cc}} \tag{2.46}$$

The whole circuit is obtained by assembling the three parts of Figs. 2.20, 2.21 and 2.22, so that the electronic circuit equivalent to the Rössler system is the circuit shown in Fig. 2.23. We notice that $C_1 R_6 = C_2 R_{12} = C_3 R_{21}$ so that the time scaling is coherent for all the equations of the set. Once designed the Rössler circuit scheme, it is checked through a circuital simulation tool, to verify that the trends of state variables are in agreement with the theoretical expectations.

Third step

In this final step, the Rössler circuit is physically implemented with low-cost components and welded on a predrilled board as shown in Fig. 2.24. The circuit is powered by a voltage generator and an oscilloscope is used to analyze the circuit behavior: the typical Rössler attractor shown in Fig. 2.25 is found. To compensate for all the component tolerances and to reproduce the different behaviors of the Rössler circuit it might be necessary to change the parameter c, which can be suitably accomplished by varying the value of the resistor R_{25}. A variable resistor, i.e., a trimmer, is then used substituting R_{25}.

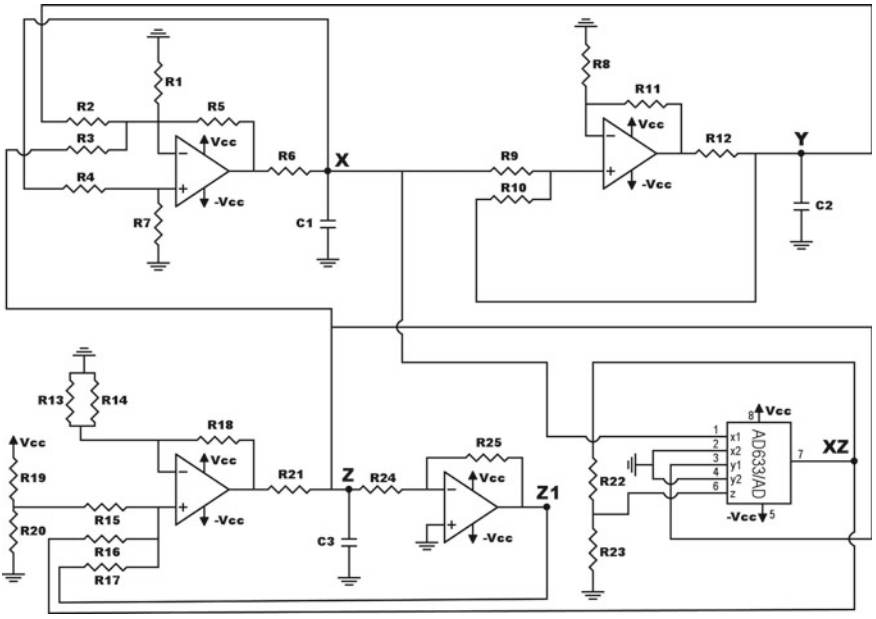

Fig. 2.23 Scheme of the electronic circuit equivalent to the Rössler system

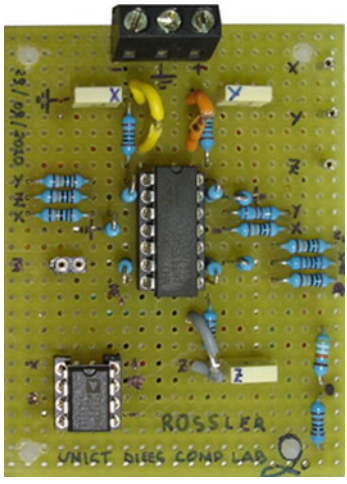

Fig. 2.24 A picture of the implemented Rössler circuit

2.4 Implementation Through FPAA

Field Programmable Analog Arrays (FPAAs) provide an alternative way to implement chaotic circuits, following the same approach described in Sect. 2.2, but using, instead of components to be mounted on a development board, the blocks which are

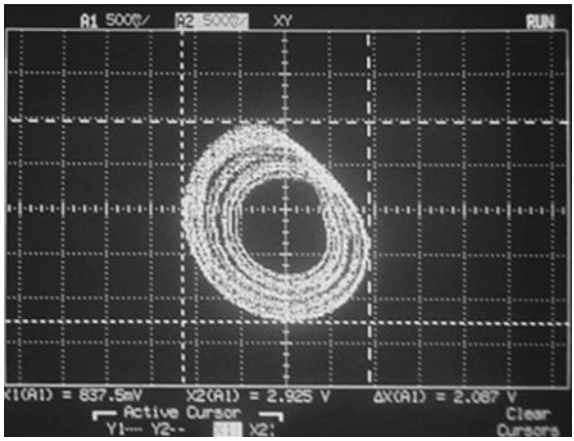

Fig. 2.25 Experimental attractor of the Rössler circuit. *Phase plane* $X-Y$, *horizontal axis* 500 mV/div, *vertical axis* 500 mV/div

already contained in such programmable analog device. In fact, FPAAs represent the analog counterpart of Field Programmable Gate Array (FPGA) and contain a matrix of Configurable Analog Blocks (named CABs) that can be connected with each other and with external I/O blocks. Each CAB typically contains digital and analog comparators, some operational amplifiers and a series of capacitors. The FPAA technology is, in fact, mainly based on switched capacitor technology. The CAB blocks are surrounded by the other elements of the device, dedicated to clock management, signal I/O and block configuration, and dynamic reprogrammability. Some device can be also connected to external microcontroller to offer on-the-fly dynamic reprogrammability of the parameter values. Typical CABs are: inverting gain block, integrators, analog filters, algebraic adders. An FPAA in practice contains the fundamental blocks which are needed for an implementation based on the procedure of Sect. 2.2. The design can be done following the same guidelines, by taking into account the voltage supply limits which now depend on the specific hardware equipment used.

Using FPAA it is possible to reprogram the entire circuit dynamics, keeping the structure fixed but changing the parameters. The reprogrammability features of FPAA can also be used to adapt the circuit to changing external conditions due to noise or changes in the operating conditions of the system being controlled. The circuit configurations can be changed at a low level, where components such as operational amplifiers, capacitors, resistors, transconductors, and current mirrors can easily be fixed and connected, and also at a high level. In the latter case, user-friendly tools are often made available by the producers of the devices in order to reduce the time to market for products.

The two main characteristics of FPAA are the possibility to translate complex analog circuits into a set of low-level functions and the capability to place analog circuits under real-time software control within the system. For these reasons FPAA provides an interesting approach to implement chaotic circuits with programmable features. Examples of the use of FPAA for chaotic circuit implementations will be provided in Chap. 4.

References

1. Sedra AS, Smith KC (2003) Microelectronic circuits. Oxford University Press, Oxford
2. Fortuna L, Rizzo A, Xibilia MG (2003) Modeling complex dynamics via extended PWL-based CNNs. Int J Bifurcat Chaos 13(11):3273–3286
3. Xia Y, Fu M, Shi P (2009) Analysis and synthesis of dynamical systems with time-delays. Lecture notes in control and information sciences. Springer, New York
4. Ikeda K, Matsumoto K (1987) High-dimensional chaotic behavior in systems with time-delayed feedback. Physica D 29:223–235
5. Rossler OE (1976) An equation for continuous chaos. Phys Lett A 57(5):397–398

http://www.springer.com/978-3-319-05899-3

A Concise Guide to Chaotic Electronic Circuits

Buscarino, A.; Fortuna, L.; Frasca, M.; Sciuto, G.

2014, VIII, 100 p. 115 illus., 23 illus. in color., Softcover
ISBN: 978-3-319-05899-3